MoorDyn V2: New Capabilities in Mooring System Components and Load Cases

Preprint

Matthew Hall

National Renewable Energy Laboratory

Presented at the ASME 2020 39th International Conference on Ocean, Offshore and Arctic Engineering
August 3–7, 2020

NREL is a national laboratory of the U.S. Department of Energy
Office of Energy Efficiency & Renewable Energy
Operated by the Alliance for Sustainable Energy, LLC

This report is available at no cost from the National Renewable Energy Laboratory (NREL) at www.nrel.gov/publications.

Contract No. DE-AC36-08GO28308

Conference Paper
NREL/CP-5000-76555
September 2020

MoorDyn V2: New Capabilities in Mooring System Components and Load Cases

Preprint

Matthew Hall

National Renewable Energy Laboratory

Suggested Citation
Hall, Matthew. 2020. *MoorDyn V2: New Capabilities in Mooring System Components and Load Cases: Preprint*. Golden, CO: National Renewable Energy Laboratory. NREL/CP-5000-76555. https://www.nrel.gov/docs/fy20osti/76555.pdf.

Conference Paper
NREL/CP-5000-76555
September 2020

National Renewable Energy Laboratory
15013 Denver West Parkway
Golden, CO 80401
303-275-3000 • www.nrel.gov

NOTICE

This work was authored by the National Renewable Energy Laboratory, operated by Alliance for Sustainable Energy, LLC, for the U.S. Department of Energy (DOE) under Contract No. DE-AC36-08GO28308. Funding provided by the U.S. Department of Energy Office of Energy Efficiency and Renewable Energy Wind Energy Technologies Office. The views expressed herein do not necessarily represent the views of the DOE or the U.S. Government. The U.S. Government retains and the publisher, by accepting the article for publication, acknowledges that the U.S. Government retains a nonexclusive, paid-up, irrevocable, worldwide license to publish or reproduce the published form of this work, or allow others to do so, for U.S. Government purposes.

Cover Photos by Dennis Schroeder: (clockwise, left to right) NREL 51934, NREL 45897, NREL 42160, NREL 45891, NREL 48097, NREL 46526.

MOORDYN V2: NEW CAPABILITIES IN MOORING SYSTEM COMPONENTS AND LOAD CASES

Matthew Hall
National Renewable Energy Laboratory
Golden, Colorado, USA

ABSTRACT

MoorDyn, an open-source mooring dynamics model, is being expanded with capabilities for additional mooring system features and load cases. As floating wind turbine technology matures, mooring systems are becoming more sophisticated and more complex scenarios need to be considered in the design process. Mooring systems may have synthetic line materials, ballast/buoyancy bodies along the lines, or interconnections between platforms. Failure modes may involve multiple cascading line failures that depend on mooring system dynamics.

Features recently added to MoorDyn aim to address these emerging needs. MoorDyn's linear elasticity model has been supplemented to support user-defined stress-strain curves, which can be adjusted to represent synthetic mooring materials. Rigid six-degree-of-freedom bodies in the mooring system can now be modeled using two new model objects. "Rod" objects provide an option for rigid cylindrical bodies. They use the existing Morison equation-based hydrodynamics model and can be connected to mooring lines at either end. "Body" objects provide a generic six-degree-of-freedom rigid-body representation based on a lumped-parameter model of translational and rotational properties. Rod objects can be added to Body objects and mooring lines can be attached at any location, allowing a wide variety of submerged structures to be integrated into the mooring system. Lastly, a means of dynamically simulating mooring line failures has been implemented.

These new features, currently in the C++ version of MoorDyn, are described and then demonstrated on a two-turbine shared-mooring array. A qualitative view of the results suggests the new features are functioning as expected.

INTRODUCTION

As floating wind turbine technology matures beyond single prototypes toward large commercial farms, more sophisticated mooring systems become increasingly relevant and more complex scenarios need to be considered in the design process. New mooring systems may feature synthetic line materials, weight or buoyancy bodies along the lines, and even interconnections between platforms (e.g. [1,2]). With these mooring systems, wave and current loads can be more significant, and failure cases may involve mooring failures cascading throughout a farm (e.g. [3]). These developments call for more advanced coupled mooring modeling capabilities, with expansion in both the types of systems that can be modeled and the load scenarios that they can be exposed to.

MoorDyn is a lumped-mass mooring system dynamics model that is highly accessible to researchers and designers because it is open source, easy to couple with, and included in the floating wind turbine simulator OpenFAST [4,5]. Up until this point, MoorDyn's development has prioritized efficiency and versatility over model capabilities. It uses a simple lumped-mass formulation that accounts for a mooring line's axial elasticity, hydrodynamic forces from Morison's equation, and seabed contact forces based on horizontal friction coefficients and vertical spring-damper coefficients [6]. Point-mass connection objects provide representation of line interfaces, clump weights, floats, and structural couplings with other models. These abilities allow for simulating a variety of mooring system configurations, but there are notable limitations in aspects such as nonlinear elastic properties and rigid mooring system components.

Building on the existing capabilities, a variety of new model features have been added to bring more advanced and increasingly demanded capabilities to MoorDyn. Given the significant input file expansions and code restructuring needed to accommodate these features, the resulting model is termed "version 2" to clearly distinguish it from previous versions.

This paper details the methodology and implementation of the main new features in MoorDyn v2 and then demonstrates them on a sample shared-mooring floating wind farm featuring synthetic lines, rigid bodies in the mooring system, and a line failure partway through the simulation.

MOORING LINE ELASTICITY MODEL

MoorDyn models a mooring line as a concatenation of point masses (nodes) connected by spring-dampers (segments). As detailed in [6], MoorDyn lumps all forces along a line at the node points. The forces, illustrated in Figure 1, include weight and buoyancy (W), axial stiffness (T), axial structural damping (C), hydrodynamic drag (D), and seabed contact (B).

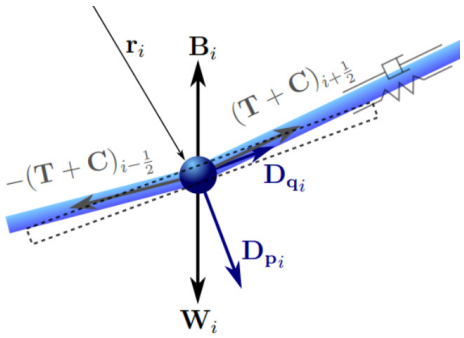

FIGURE 1: LUMPED FORCES ON A LINE NODE

Line tension is the only force that is calculated at the segments rather than at the nodes. It is calculated as

$$(T+C)_{i+\frac{1}{2}} = E\frac{\pi}{4}d^2\left(E(\epsilon)\epsilon_{i+\frac{1}{2}} + B(\dot{\epsilon})\dot{\epsilon}_{i+\frac{1}{2}}\right) \qquad (1)$$

where E is the elasticity modulus, ϵ is the segment strain, B is a structural damping coefficient, and $\dot{\epsilon}$ is the segment strain rate.

In previous versions of MoorDyn, E and C were constants. Now, as indicated by the equation, the linear elasticity model in MoorDyn has been supplemented to support a user-defined nonlinear stress-strain relationship. The quantity E can be calculated as a function of strain, ϵ, from a user-specified look-up table. This allows better representation of the quasi-static elasticity properties of synthetic mooring line materials.

As a step toward more complex elastic behavior, a rate-dependent damping coefficient lookup table has also been implemented following a similar approach. The use of a lookup-table approach for elastic properties provides some means of simulating specialized mooring elements with tuned elasticity characteristics. More advanced elasticity models that might incorporate functions of both strain and strain rate, or a hysteresis effect tracked through an elasticity-related state variable, are an area for future work.

MODELING OF RIGID BODIES

Rigid six-degree-of-freedom (6-DOF) bodies can now be modeled in the mooring system. The original approach of modeling clump weights or floats as point masses neglects the significant effect on tensions that can result from line connections being offset from a body's center of mass. Furthermore, some support structure designs involve drag devices suspended beneath a structure or within a mooring system. To account for these possibilities, MoorDyn's existing object types—Lines and Connections—have been supplemented with two new, 6-DOF object types: Rods and Bodies. (For clarity, capitalization is used to differentiate MoorDyn object types from more general uses of these words.)

General Handling of 6-DOF Objects

The introduction of 6-DOF objects adds moments to the model and requires handling of 6-by-6 matrices and transforming lumped properties to preserve both forces and moments in different reference frames. These changes require new functions in MoorDyn.

When dealing with 6-DOF objects, inertial properties need to be lumped at user-specified reference frames that may not necessarily coincide with a body's center of mass. This is especially true in the case of added mass where, unlike in a normal mass matrix, off-diagonal terms can exist because the body shape and orientation can cause acceleration in one direction to create a reaction force in another direction. Transforming full mass matrices is not commonly discussed in the literature because inertial coupling of translational DOFs is an uncommon situation. Sadeghi and Incecik [7] describe the general approach and provide the matrix transform steps.

As detailed in [7], a 6-by-6 mass matrix is composed of three unique 3-by-3 matrices: the mass matrix **M**, the product of inertia matrix **J**, and the moment of inertia matrix **I**:

$$\mathbf{M}_{6x6} = \begin{bmatrix} \mathbf{M} & \mathbf{J} \\ \mathbf{J}^{\mathrm{T}} & \mathbf{I} \end{bmatrix}. \qquad (2)$$

Any 6-DOF object in MoorDyn will require handling of this 6-by-6 matrix about its reference point when solving for its motion. Because MoorDyn does not assume the reference point is at the center of mass, and because couplings are induced by added-mass terms, there is little possibility of avoiding a full 6-by-6 matrix equation of motion:

$$\mathbf{M}_{6x6}\ddot{\mathbf{r}}_6 = \mathbf{f}_{6net}, \qquad (3)$$

where $\ddot{\mathbf{r}}_6$ is the body's 6-DOF acceleration vector (three translations and three angles), and $\mathbf{f}_{6net}$ is the corresponding vector of summed forces and moments acting on the body. To solve this efficiently, lower-upper (LU) decomposition is now used in MoorDyn's solver. Whether the rigid body in question is a Rod or a Body object, once the forces and masses are lumped at the reference point, the same 6-by-6 equation of motion solution process is used.

The following subsections describe the new Rod and Body objects.

Rod Objects

Rod objects provide an option for rigid cylindrical elements within a mooring system. They are modeled very similarly to Lines except for their lack of flexibility, which reduces their degrees of freedom to 6. Like Lines, they are divided into a number of nodes at which weight, buoyancy, seabed contact, and Morison-based hydrodynamic forces are calculated. Unlike Lines, their internal structural forces are not calculated.

The key implementation step for Rod objects is lumping the forces and masses at each node along the Rod length into a single set of 6-DOF forces and mass coefficients at the Rod reference point.

For lumping forces, combining the point force vectors, $\mathbf{f}_i$, at each node, i, along the Rod into a single force and moment vector, $\mathbf{f}_6$, at the Rod reference point is easily done using

$$\mathbf{f}_6 = \sum \begin{Bmatrix} \mathbf{f}_i \\ (\mathbf{r}_i - \mathbf{r}_{ref}) \times \mathbf{f}_i \end{Bmatrix}, \quad (4)$$

where $\mathbf{r}_i$ is each node's location in the global frame and $\mathbf{r}_{ref}$ is the location of the Rod's reference point.

Lumping the mass characteristics is less straightforward because of the off-diagonal terms provided by added mass at each node. As in MoorDyn's existing Line object model, each node has the following 3-by-3 added mass matrix:

$$\mathbf{A}_i = \rho_w \frac{\pi}{4} d^2 l \, [C_{an}(\mathbf{I} - \hat{\mathbf{q}}_i \hat{\mathbf{q}}_i^T) + C_{at} \hat{\mathbf{q}}_i \hat{\mathbf{q}}_i^T]. \quad (5)$$

The nodes' added-mass matrices need to be lumped into a single 6-by-6 added-mass matrix at the Rod's reference point. For computational simplicity, the fact that node added-mass matrices are already in the inertial frame is used to avoid a full 6-DOF transformation of the mass/inertia properties. Instead, the effect of each 3-by-3 matrix is simply translated to the Rod reference point and then summed. As detailed in [7], the transformation of mass and inertia properties about a position, $\mathbf{r}_i$, to a new reference position, $\mathbf{r}'$, is

$$\mathbf{M}' = \sum \mathbf{M}_i \quad (6)$$

$$\mathbf{J}' = \sum \mathbf{M}_i \mathbf{H}_i + \mathbf{J}_i \quad (7)$$

$$\mathbf{I}' = \sum \mathbf{H}_i \mathbf{M}_i \mathbf{H}_i^T + \mathbf{J}_i^T \mathbf{H}_i + \mathbf{H}_i^T \mathbf{J}_i + \mathbf{J}_i \quad (8)$$

where $\mathbf{H}$ is the matrix of antisymmetric tensor components defined as $H_{ij} = \epsilon_{ijk} d_k$, where $\mathbf{d} = \mathbf{r}' - \mathbf{r}$ and ϵ is the Levi-Civita (permutation) symbol.

Two types of Rods are set up in MoorDyn. Free Rods are independent bodies that have a connection point at each end, allowing any number of lines to be connected. Attached Rods are part of a Body and move rigidly with that body rather than having their own independent degrees of freedom. Attached Rods also have connection points at the ends, which can optionally be used to attach lines directly to the Rod.

Body Objects

Body objects provide a generic 6-DOF rigid-body representation based on a lumped-parameter model of translational and rotational properties (e.g. hydrodynamic drag and added-mass coefficients). Rod objects can be added to a Body and mooring lines can be attached via Connection objects at any location on a Body, allowing a wide variety of submerged structure geometries to be integrated into the mooring system. Separate from force and mass contributions that might come from incorporated Rod objects or attached Connection and Line objects, the core Body object properties are as follows:

- Mass and center of mass,
- Volumetric displacement (assumed to be at reference point),
- Mass moment of inertia about each axis,
- Hydrodynamic drag coefficient in each direction,
- Rotational hydrodynamic drag coefficient about each axis,
- Added-mass coefficient in each direction,
- Added-mass moment of inertia coefficient about each axis.

These properties are used to form the Body's 6-by-6 matrix equation of motion coefficients. Because the Body has direction-specific coefficients, a full 6-DOF transformation is needed to create the final equation of motion. As discussed in [7], because **M**, **J**, and **K** are second-order tensors, they can each be transformed to a new coordinate system orientation using a direction cosine matrix, **A**:

$$\mathbf{M}' = \mathbf{A}\mathbf{M}\mathbf{A}^{\mathrm{T}} \quad (9)$$

$$\mathbf{J}' = \mathbf{A}\mathbf{J}\mathbf{A}^{\mathrm{T}} \quad (10)$$

$$\mathbf{I}' = \mathbf{A}\mathbf{I}\mathbf{A}^{\mathrm{T}} \quad (11)$$

Transformations for any offsets are handled using the equations (6-8) discussed for Rod objects.

MODEL STRUCTURE AND FAILURE SIMULATION

The addition of two new object types, with multiple ways of relating to other objects, necessitated creating a well-defined object hierarchy in MoorDyn. This hierarchy is shown in Figure 2. It is organized from the top down in terms of which object types can set the kinematics of other object types. From the bottom up, the hierarchy describes which objects can apply reaction forces onto other objects.

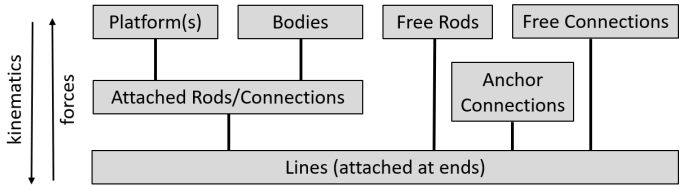

FIGURE 2: MOORDYN V2 OBJECT HIERARCHY

Figure 2 indicates the various connections between object types that are possible. At each time-integration step, the latest state variable values are fed into the mooring system "top-down", first from the externally modeled floating platform, through its attached fairlead Connections, then into attached Line ends. Similarly, Body objects, which track their own states, pass their kinematics to attached Rod and Connection objects, and through them to any attached Line ends. Free Rod objects, which track their own states, pass their end kinematics to the ends of attached Lines. Free Connection objects pass kinematics to attached Line ends, as always. The calculation of forces and resulting state derivatives is done in the opposite direction: from Lines, to Connections or Rods, to Bodies and/or the coupled platform. There can be multiple coupled platforms, as discussed in previous work [8].

In the process of adding new model objects, a means of simulating mooring line failures was identified. This method,

which can be triggered either by a timer or a tension threshold, works by adding a new massless Connection object at the location of a line failure. This massless Connection preserves the physics of the line as though its end had been severed from the attachment point. The limitation of this approach is that failures can only occur where Connections already exist. When the failure occurs, the Line that has failed is removed from the Connection and its end is instead fitted with the new zero-mass Connection. By inserting Connections at anticipated failure points, failures can be simulated at any predetermined location within the mooring system.

Figure 3 illustrates how a failure would be modeled at a certain point along a line. A massless Connection object that is used to connect two separate Lines is converted into two separate Connections—one for each Line—to simulate the failure.

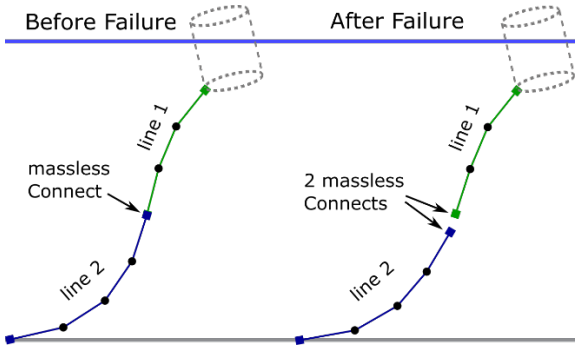

FIGURE 3: SIMULATION OF MID-LINE FAILURE

For more complex mooring systems, such as in shared-mooring floating wind farms, the tension-threshold-based line failure capability allows dynamic simulation of cascading failures within a mooring system.

DEMONSTRATION SCENARIO

MoorDyn's new capabilities are demonstrated through simulation of a shared mooring system for two floating wind turbines that includes cylindrical weight and buoyancy bodies along the shared mooring line. The configuration is illustrated in Figure 4. The water depth is 200 m, the turbine spacing is 600 m, and the floating wind turbines match the description of the OC4-DeepCwind semisubmersible [9] with the National Renewable Energy Laboratory (NREL) 5-MW reference turbine [10].

The buoyancy body ("F") shown in the middle of the illustration is modeled in MoorDyn as a free Rod object. The two weight bodies ("W") on either side are modeled as Bodies each composed of two attached Rods, one for the main cylinder and one for a thin heave plate at the bottom. The general component properties are given in Table 1.

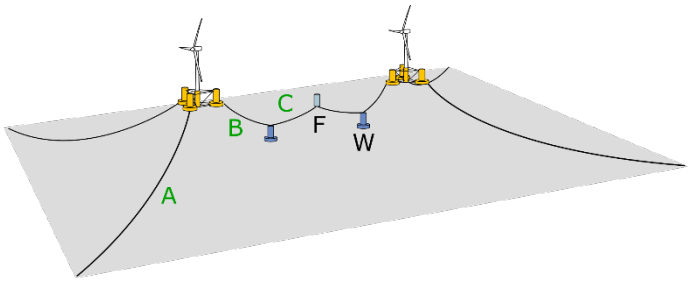

FIGURE 4: DEMONSTRATION MOORING SYSTEM

The anchored mooring lines ("A") are chains with the same layout and specifications as the OC4-DeepCwind semisubmersible's moorings [9]. The shared mooring lines running between the platforms ("B" and "C") are synthetic rope with a diameter of 96 mm diameter, a linear density of 590 g/m, and a nonconstant stiffness as indicated in Figure 5. This stiffness curve is intended to demonstrate the new nonlinear elasticity capability rather than specifically match certain mooring material properties. The constant chain stiffness is also plotted for comparison. The mooring line properties and lengths are given in Table 2.

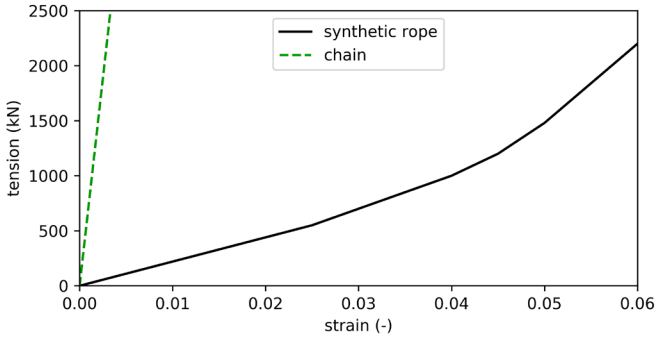

FIGURE 5: LINE STIFFNESS CURVES

TABLE 1: MOORING BODY PROPERTIES

Object label	W	F
Diameter (m)	2.0	3.6
Height (m)	4.0	6.0
Mass (t)	120	12
Heave plate diameter (m)	4.0	N/A

TABLE 2: MOORING SYSTEM PROPERTIES

Line type label	A	B	C
Effective diameter (mm)	76.6	96	96
Unstretched length (m)	835	150	134
Linear density (kg/m)	113	0.59	0.59
Stiffness (MN)	753	Variable	Variable

The floating wind turbines coupled to the mooring system are modeled by interfacing MoorDyn v2 with two FAST v7 simulations using the methodology described in [11]. An overview of the approach, which involves using a master

program to connect MoorDyn and FAST simulations and provide precalculated wave loads, is shown in Figure 6.

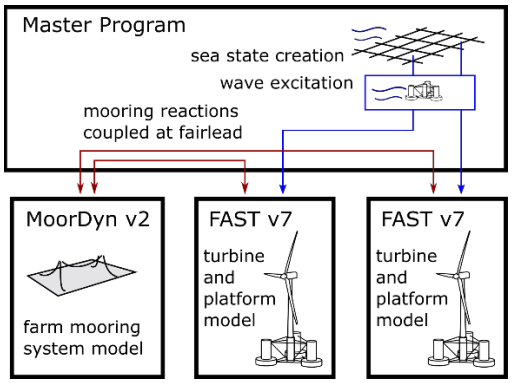

FIGURE 6: COUPLED MODELING APPROACH

During simulation, the master program routes information about the platform motions and mooring system reactions between FAST and MoorDyn. FAST models the dynamics of each floating wind turbine, from platform hydrodynamics to turbine aeroelastics.

The model is demonstrated with a turbulent wind and irregular waves case based on LC 3.2 of OC4 Phase II [12]. The sea state is a 10-s, 6-m JONSWAP spectrum. The winds have a mean speed of 11.4 m/s and Class B turbulence levels. Proper phasing of wave loads on each turbine based on their spacing in the array is preserved. Wind conditions are randomized between the two turbines, which are spaced 5 rotor diameters apart, and wake effects are neglected for the purposes of the current work. Wind and waves are aligned with the turbine pair.

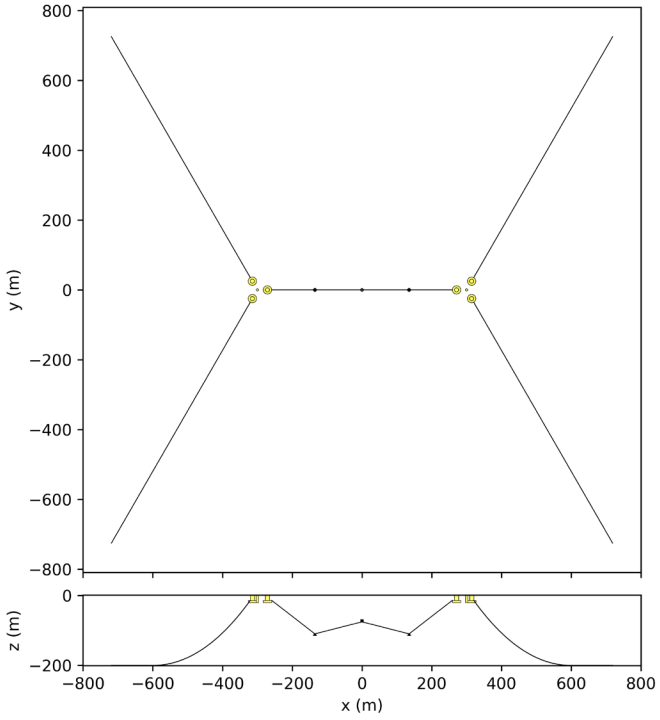

FIGURE 7: EQUILIBRIUM MOORING CONFIGURATION

RESULTS

The mooring system was tuned to hold the desired turbine spacing at equilibrium while keeping the shared line elements a safe distance from the seabed and sea surface. Figure 7 shows the mooring configuration at equilibrium.

A 10-minute simulation of the stochastic wind and wave load case was run to demonstrate the new MoorDyn features. Figures 8 and 9 show the general stationkeeping behavior of the shared mooring system in terms of surge motions and mooring component depths, respectively. The surge offsets shown in Figure 8 demonstrate the spreading that occurs in the shared-mooring array because the restoring force is distributed throughout the mooring system, resulting in the downwind turbine and mooring system components having the greatest offsets. The change in depths of the weights and the float along the shared mooring line shown in Figure 9 reveals how the shared line becomes straighter and rises in the water column as its tension increases because of the turbines spreading.

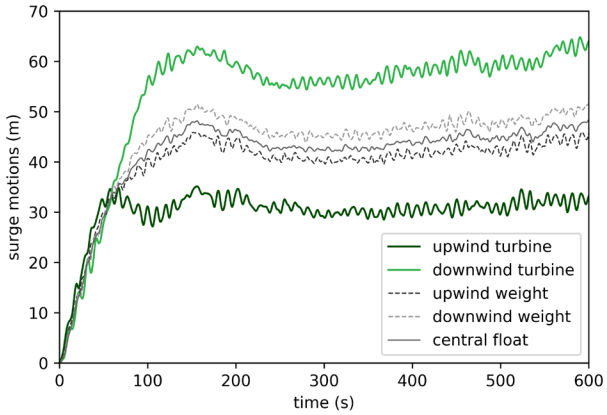

FIGURE 8: PLATFORM/BODY SURGE RESPONSES

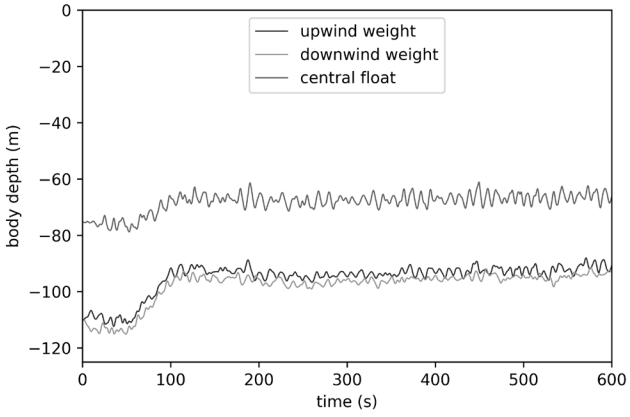

FIGURE 9: SHARED-LINE BODY DEPTHS

It is also notable in the response to the turbine thrust forces shown in Figures 8 and 9 that the most upwind body reaches its equilibrium surge offset first, followed by the next most upwind body, and so on.

Figures 10-12 plot 60 s excerpts of platform and body heave responses, platform and body pitch responses, and tensions along the shared mooring line to show the system's behavior in the wave frequency range. The heave responses shown in Figure 10 reveal that the bodies along the shared mooring line have significantly larger heave amplitudes than the floating platforms. This can be explained by the shallow incline angle of the shared line segments, which results in the body heave motions being affected significantly by platform surge motions, particularly when the two platforms surge out of phase with each other. The irregular shapes of the body heave time series suggest that this shared mooring system is reasonably hydrodynamically damped rather than resonating at its own natural frequency. This also suggests that the drag modeled by MoorDyn's new Rod objects is producing the desired behavior, at least qualitatively.

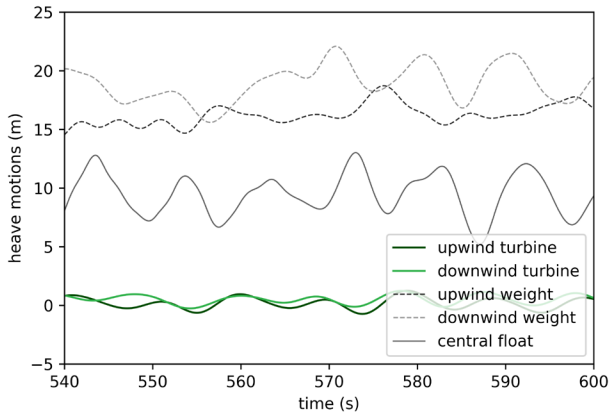

FIGURE 10: PLATFORM/BODY HEAVE RESPONSES

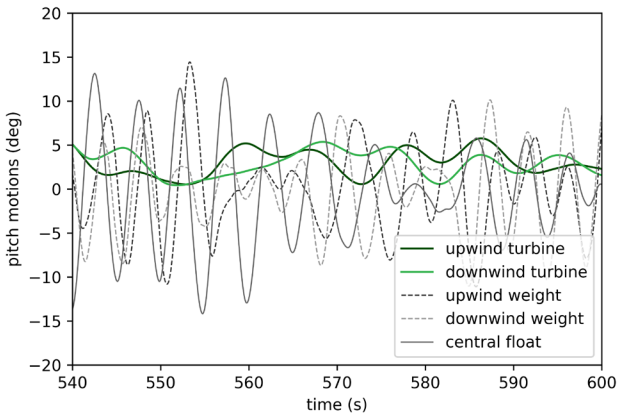

FIGURE 11: PLATFORM/BODY PITCH RESPONSES

The pitch responses shown in Figure 11 indicate that the bodies along the shared mooring line have larger pitch motions at noticeably higher frequencies than the platform pitch motions. This increased response is somewhat expected given the small dimensions of these bodies relative to the turbine platforms and their single-point attachments to the mooring line, which allows them to rotate freely. However, the relatively undamped appearance of the weights' pitch responses, when they have heave plates, suggests that the lack of drag moment modeling at Rod ends may be significant for this situation.

Figure 12 shows the tensions at four points along the shared mooring line: the two ends where the line attaches to the turbine platforms, and the two points where line segments attach to the central float. Although the mean tensions at all four points are relatively similar, trends can be observed. Most notably, the upwind half of the shared line has significantly higher tension amplitudes than the downwind half. The reasons for this are yet to be determined, although it seems likely that the higher tensions on the upwind anchor lines may result in more severe platform motions on the upwind platform, which would translate into more severe dynamic mooring loads on attached lines.

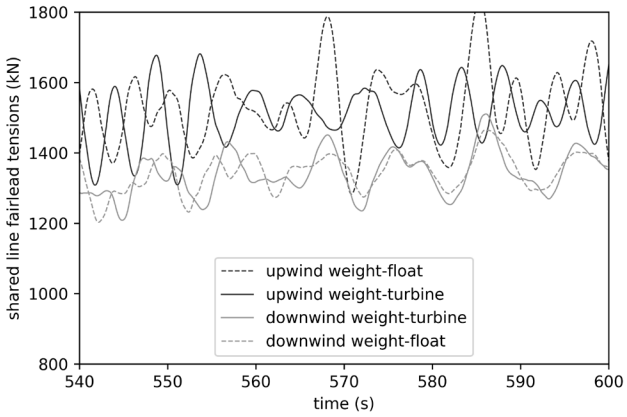

FIGURE 12: TENSIONS ALONG THE SHARED LINE

Failure Demonstration

To demonstrate the new line failure capability, the previously described load case is repeated with the introduction of a failure. A massless connection is added in the upwind line between the weight and float 31 m from the float, and a failure is triggered at this connection 300 s into the simulation. Figure 13 shows snapshots of the positions of the shared mooring components for 2.5 s following the failure. The snapshots show rapid shortening of the line once it fails, followed by the more gradual initiation of large motions by the attached bodies. Later in the simulation, the floating wind turbine platforms begin to drift apart.

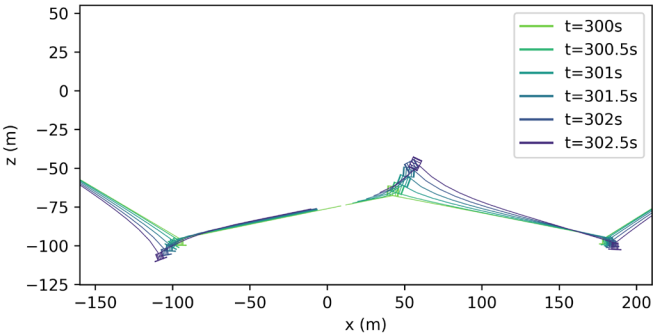

FIGURE 13: SHARED LINE FAILURE SNAPSHOTS

Figures 14-16 show how the platforms and bodies move in surge, heave, and pitch once the line failure occurs. The original no-failure results are shown in green or grey, and the with-failure results are shown in red.

Figure 14 shows the bodies on the shared line rapidly moving apart horizontally once the failure occurs, followed by the floating platforms diverging more slowly. Figure 15 shows the float rising and the weights falling once the failure occurs, along with changes in the floating platforms' heave responses as a result of the change in mooring system reaction forces. Figure 16 shows how the failure induces dramatic pitch motions in the attached bodies. The bodies attached to the failed line maintain a large pitch angle for an extended time as they swing toward their new equilibrium positions—a consequence of the moment induced by their remaining connected line's attachment location. As with heave, the platforms' pitch responses are somewhat altered by the change in mooring system reaction forces.

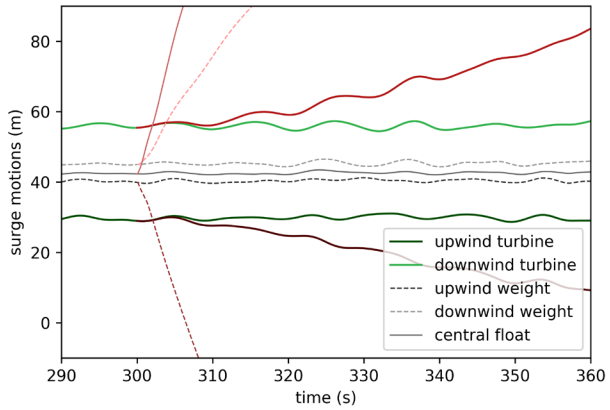

FIGURE 14: SURGE RESPONSES AFTER FAILURE

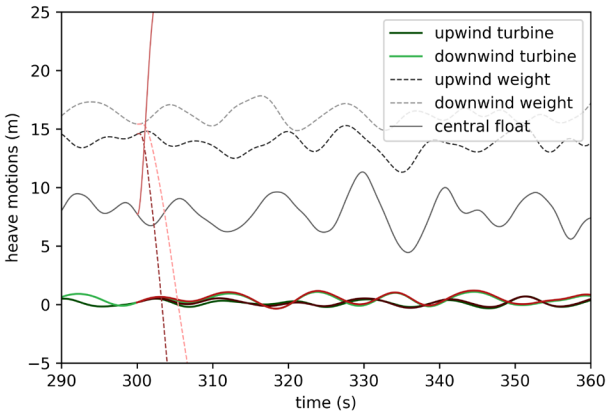

FIGURE 15: HEAVE RESPONSES AFTER FAILURE

Figure 17 shows the tensions at the upper ends of the shared line segments following the failure. The tension of the failed line segment drops to zero nearly instantly as expected because it is synthetic and neutrally buoyant. The tensions of the other lines also fall as the shared system loses its horizontal tension. In contrast, the upwind line from the platform to the weight regains a large part of its tension as the weight comes to rest and hangs from this single line.

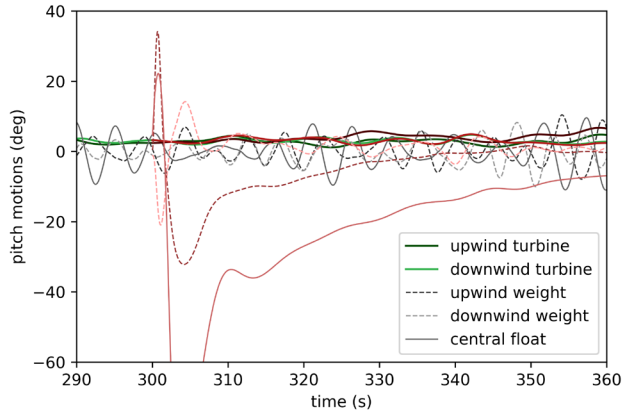

FIGURE 16: PITCH RESPONSES AFTER FAILURE

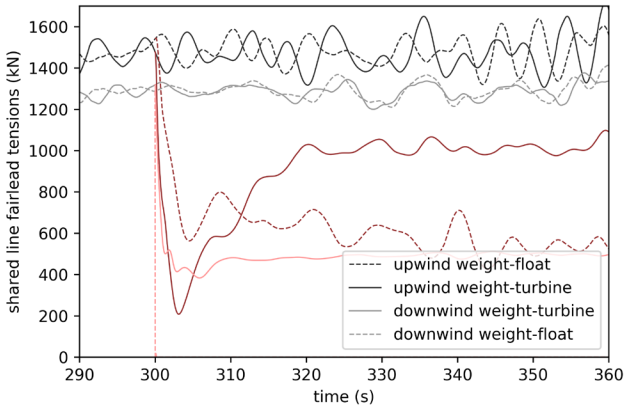

FIGURE 17: SHARED LINE TENSIONS AFTER FAILURE

CONCLUSION

A new version of MoorDyn has been developed that significantly expands the range of scenarios that can be modeled. Nonlinear elasticity characteristics have been implemented using a look-up table approach, facilitating simulation of synthetic line materials. Rigid cylindrical Rod objects have been introduced, which provide modeling of Morison-equation-based distributed loads in 6 degrees of freedom. Generic lumped-parameter 6-DOF Body objects have been introduced, which allow handling of various objects within the mooring system that have rotational inertia. In addition, Rods can be added to Bodies to provide modeling of more complex structures suspended within the mooring system.

To accommodate the additional model components, the object hierarchy in MoorDyn was revised. A way to model mooring line failures was developed based on mid-simulation creation of zero-mass Connection objects. This capability allows realistic dynamic modeling of failure events, triggered by either time or tension limits.

These new features have been demonstrated by simulating a hypothetical shared mooring system created for this purpose. Coupled simulation of MoorDyn v2 with FAST v7 shows MoorDyn's new features, including line failure, to be operating reasonably in the simulated scenario, at least to a qualitative degree. One caveat is that neglecting modeling of rotational damping at Rod ends may be significant when using short Rod objects to model a heave plate. Exploring this issue and moving on to more quantitative verification of the new model features are important next steps.

Altogether, the discussed features show promise in enabling simulation of more advanced mooring systems and dynamic failure cases. It should be noted that, at the time of writing, these improvements have only been implemented in the C++ version of MoorDyn. Implementation in MoorDyn F, which is coupled with OpenFAST, will be done after verification is completed.

ACKNOWLEDGEMENTS

This work was authored by the National Renewable Energy Laboratory, operated by the Alliance for Sustainable Energy, LLC, for the U.S. Department of Energy (DOE) under Contract No. DE-AC36-08GO28308. The views expressed in the article do not necessarily represent the views of the DOE or the U.S. Government. The U.S. Government retains and the publisher, by accepting the article for publication, acknowledges that the U.S. Government retains a nonexclusive, paid-up, irrevocable, worldwide license to publish or reproduce the published form of this work, or allow others to do so, for U.S. Government purposes.

REFERENCES

[1] P. Connolly and M. Hall, "Comparison of Pilot-Scale Floating Offshore Wind Farms with Shared Moorings," *Ocean Engineering*, vol. 171, pp. 172–180, 2018.

[2] C. M. Fontana, S. R. Arwade, D. J. DeGroot, A. T. Myers, M. Landon, and C. Aubeny, "Efficient Multiline Anchor Systems for Floating Offshore Wind Turbines," in *Proceedings of the 35th International Conference on Ocean, Offshore and Arctic Engineering*, Busan, South Korea, Jun. 2016.

[3] S. T. Hallowell *et al.*, "System reliability of floating offshore wind farms with multiline anchors," *Ocean Engineering*, vol. 160, pp. 94–104, 2018.

[4] M. T. Andersen, F. T. Wendt, A. N. Robertson, J. M. Jonkman, and M. Hall, "Verification and Validation of Multisegmented Mooring Capabilities in FAST v8," in *Proceedings of the Twenty-sixth International Offshore and Polar Engineering Conference*, Rhodes, Greece, 2016.

[5] J. Jonkman and M. Sprague, "OpenFAST | NWTC Information Portal." https://nwtc.nrel.gov/openfast (accessed Jan. 01, 2020).

[6] M. Hall and A. Goupee, "Validation of a lumped-mass mooring line model with DeepCwind semisubmersible model test data," *Ocean Engineering*, vol. 104, pp. 590–603, 2015.

[7] K. Sadeghi and A. Incecik, "Tensor Properties of Added-mass and Damping Coefficients," *Journal of Engineering Mathematics*, vol. 52, no. 4, pp. 379–387, Aug. 2005.

[8] M. Hall, "Efficient Modelling of Seabed Friction and Multi-Floater Mooring Systems in MoorDyn," in *Proceedings of the 12th European Wave and Tidal Energy Conference*, Cork, Ireland, Aug. 2017.

[9] A. Robertson *et al.*, "Definition of the Semisubmersible Floating System for Phase II of OC4," National Renewable Energy Laboratory, Golden, Colorado, USA, NREL Technical Report TP-5000-60601, 2014.

[10] J. M. Jonkman, S. Butterfield, W. Musial, and G. Scott, "Definition of a 5-MW Reference Wind Turbine for Offshore System Development," National Renewable Energy Laboratory, Golden, Colorado, NREL Technical Report TP-500-38060, 2009.

[11] M. Hall and P. Connolly, "Coupled Dynamics Modelling of a Floating Wind Farm with Shared Moorings," in *ASME 2018 37th International Conference on Ocean, Offshore and Arctic Engineering*, Madrid, Spain, Jun. 2018.

[12] A. Robertson *et al.*, "Offshore Code Comparison Collaboration Continuation Within IEA Wind Task 30: Phase II Results Regarding a Floating Semisubmersible Wind System," in *Proceedings of the 33rd International Conference on Ocean, Offshore and Arctic Engineering*, San Francisco, California, USA, Jun. 2014.